Journal of Zhejiang University-SCIENCE B (Biomedicine & Biotechnology)
ISSN 1673-1581 (Print); ISSN 1862-1783 (Online)
www.jzus.zju.edu.cn; www.springerlink.com
E-mail: jzus@zju.edu.cn

Comparative transcriptomic analysis of vascular endothelial cells after hypoxia/re-oxygenation induction based on microarray technology*#

Jia XU[1,2,3], Jiu-kun JIANG[1,2,3], Xiao-lin LI[1,2,3], Xiao-peng YU[4], Ying-ge XU[1,2,3], Yuan-qiang LU†‡[1,2,3]

[1]*Department of Emergency Medicine, the First Affiliated Hospital, School of Medicine, Zhejiang University, Hangzhou 310003, China*

[2]*Department of Geriatric Medicine, the First Affiliated Hospital, School of Medicine, Zhejiang University, Hangzhou 310003, China*

[3]*Zhejiang Provincial Key Laboratory for Diagnosis and Treatment of Aging and Physic-chemical Injury Diseases, the First Affiliated Hospital, School of Medicine, Zhejiang University, Hangzhou 310003, China*

[4]*State Key Laboratory for Diagnosis and Treatment of Infectious Diseases, the First Affiliated Hospital, School of Medicine, Zhejiang University, Hangzhou 310003, China*

†E-mail: luyuanqiang@zju.edu.cn

Received Feb 5, 2020; Revision accepted Mar. 11, 2020; Crosschecked Mar. 11, 2020; Published online Mar. 22, 2020

Abstract: Objective: To provide comprehensive data to understand mechanisms of vascular endothelial cell (VEC) response to hypoxia/re-oxygenation. Methods: Human umbilical vein endothelial cells (HUVECs) were employed to construct hypoxia/re-oxygenation-induced VEC transcriptome profiling. Cells incubated under 5% O_2, 5% CO_2, and 90% N_2 for 3 h followed by 95% air and 5% CO_2 for 1 h were used in the hypoxia/re-oxygenation group. Those incubated only under 95% air and 5% CO_2 were used in the normoxia control group. Results: By using a well-established microarray chip consisting of 58 339 probes, the study identified 372 differentially expressed genes. While part of the genes are known to be VEC hypoxia/re-oxygenation-related, serving as a good control, a large number of genes related to VEC hypoxia/re-oxygenation were identified for the first time. Through bioinformatic analysis of these genes, we identified that multiple pathways were involved in the reaction. Subsequently, we applied real-time polymerase chain reaction (PCR) and western blot techniques to validate the microarray data. It was found that the expression of apoptosis-related proteins, like pleckstrin homology-like domain family A member 1 (PHLDA1), was also consistently up-regulated in the hypoxia/re-oxygenation group. STRING analysis found that significantly differentially expressed genes *SLC38A3*, *SLC5A5*, *Lnc-SLC36A4-1*, and *Lnc-PLEKHJ1-1* may have physical or/and functional protein–protein interactions with PHLDA1. Conclusions: The data from this study have built a foundation to develop many hypotheses to further explore the hypoxia/re-oxygenation mechanisms, an area with great clinical significance for multiple diseases.

Key words: Human umbilical vein endothelial cells (HUVECs); Hypoxia; Re-oxygenation; Microarray; Pleckstrin homology-like domain family A member 1 (PHLDA1); Long non-coding RNA (lncRNA)
https://doi.org/10.1631/jzus.B2000043 **CLC number:** R592

---

‡ Corresponding author

* Project supported by the National Natural Science Foundation of China (Nos. 81801572 and 81272075), the Foundation of Key Discipline Construction of Zhejiang Province for Traditional Chinese Medicine (No. 2017-XKA36), the Foundation of Key Research Project of Zhejiang Province for Traditional Chinese Medicine (No. 2019ZZ014), the Medical and Health Science Foundation of Zhejiang Province (No. 2019327552), the Key Research and Development Program of Zhejiang Province (No. 2019C03076), the General Research Program of Zhejiang Provincial Department of Medical and Health (No. 2013KYA066), the Opening Foundation of State Key Laboratory for the Diagnosis and Treatment of Infectious Diseases (Nos. 2018KF02 and 2019KF06), and the Program of Education Department of Zhejiang Province (No. Y201738150), China

Electronic supplementary materials: The online version of this article (https://doi.org/10.1631/jzus.B2000043) contains supplementary materials, which are available to authorized users

ORCID: Yuan-qiang LU, https://orcid.org/0000-0002-9057-4344

1 Introduction

Vascular endothelial cells (VECs) function as a barrier and active tissue in the inner layer of blood vessels, and play an important role in the reaction of organ ischemia, hypoxia, and inflammatory immunity. VECs participate in the regulation of many important balances by secreting a variety of active substances and regulating organ blood flow and coagulation, leukocyte and platelet activity (Nallamshetty et al., 2013; Lim To et al., 2015; Baldea et al., 2018). It has been reported that the endothelial cells seem to provide better hypoxia tolerance than many other cells (Filippi et al., 2018), and the relatively full extent VEC gene expression induced by hypoxia has been established (Urbanek et al., 2014; Sun et al., 2015; Wu et al., 2015; Tang et al., 2016; Baldea et al., 2018).

However, hypoxia/re-oxygenation is the common feature and may have more adverse consequences in many physiological and pathological processes, such as inflammation, obstructive sleep apnea, diabetes, atherosclerosis, myocardial infarction, ischemic stroke, pulmonary embolism, shock, cardiac arrest, cardiac pulmonary bypass, organ transplantation, and tumorigenesis (Atkeson et al., 2009; Shay and Celeste Simon, 2012; Bader et al., 2015; Pan J et al., 2015; Jiang et al., 2017; Xie et al., 2017; Li F et al., 2018; Li WY et al., 2018; Wang et al., 2018; Zhang et al., 2018; Pan H et al., 2019). In contrast to general belief, VEC hypoxia/re-oxygenation injury has recently been identified as a driver rather than a bystander to result in the possible development of organ dysfunction (Carden and Granger, 2000). So far, increased free radical generation and excessive activation of inflammatory responses are considered as important pathogeneses of endothelial hypoxia/re-oxygenation injury (Shay and Celeste Simon, 2012; Wu et al., 2015; Tang et al., 2016; Ferrucci et al., 2018; Filippi et al., 2018; Taylor et al., 2018; Haybar et al., 2019). It is a potentially serious problem, but the detailed physiological processes and transcriptome profiling of VECs after exposure to hypoxia/re-oxygenation have not yet been elucidated.

The present research is the first to focus on the comprehensive gene expression of hypoxia/re-oxygenation-induced human umbilical vein endothelial cells (HUVECs) using a microarray technique.

2 Materials and methods

2.1 Cell lines and cell culture

HUVECs were kindly provided by Procell Life Science & Technology Co., Ltd. (Wuhan, China). High-glucose Dulbecco's modified Eagle medium (DMEM; Thermo Fisher Scientific, Shanghai, China) had 10% (0.1 g/mL) fetal bovine serum (Biological Industries Israel Beit Haemek Ltd., Beit Haemek, Israel), and 100 U/mL streptomycin and 100 U/mL penicillin (Genom, Hangzhou, China) added were used for cell culture. Before being induced by hypoxia/re-oxygenation, cells in all groups were replaced with fresh medium at 37 °C under 5% CO_2 and 95% air for 12 h. Then, HUVECs in the hypoxia group were incubated under 5% O_2, 5% CO_2, and 90% N_2 by 3131 Single Tri-gas 184L incubator (Thermo Fisher Scientific) for 3 h (Niu et al., 2019); HUVECs in the hypoxia/re-oxygenation group were incubated under 5% O_2, 5% CO_2, and 90% N_2 for 3 h followed by 95% air and 5% CO_2 for 1 h; HUVECs in the normoxia group were cultured under 95% air and 5% CO_2.

2.2 Construction of transcriptome profile

Agilent SurePrint G3 Human Gene Expression v3 Microarray (8×60K; Design ID 072363, Agilent, Palo Alto, CA, USA) was used for the construction of transcriptome profiling. Each of three samples from the hypoxia/re-oxygenation and normoxia groups was used for the microarray experiment. Total RNA was extracted using TRIzol (Life Technologies, Waltham, MA, USA), quantified using the NanoDrop ND-2000 (Thermo Fisher Scientific), and assessed for integrity using Agilent Bioanalyzer 2100 (Agilent Technologies, Santa Clara, CA, USA) following the manufacturer's instructions. Total RNA (0.2 μg) of each sample was used for library construction based on the manufacturer's standard protocols. The Agilent Scanner G2505C (Agilent Technologies) was used for array scanning. Feature Extraction software (Version 10.7.1.1, Agilent Technologies) was used to extract raw data by reading array images.

2.3 Analysis of microarray raw data

The software GeneSpring (Version 13.1, Agilent Technologies) was employed to normalize the raw data with the quantile algorithm. The probes that at least 100% of the values in any one out of all conditions

have flags in "Detected" were chosen for differentially expressed gene analysis. Fold change of ≥2.0 and *P* value of ≤0.05 calculated with the *t*-test were used as the threshold set to identify a differentially expressed gene. Afterwards, Gene Ontology (GO) analysis and Kyoto Encyclopedia of Genes and Genomes (KEGG) analysis were applied to explore the potential functions and pathways of these differentially expressed genes. Fold enrichment of GO/KEGG analysis=(list hits/list total)/(population hits/population total), where "list hits" is the number of differentially expressed genes annotated to each GO/KEGG entry, "list total" is the number of differentially expressed genes involved in GO/KEGG analysis, "population hits" is the number of genes in whole microarray annotated to each GO/KEGG entry, and "population total" is the number of genes in whole microarray involved in GO/KEGG analysis. $P \leq 0.05$ indicates significant enrichment. The distinguishable gene expression pattern among samples was established by hierarchical clustering. The raw and normalized data have been submitted to the National Center of Biotechnology Information (NCBI) Gene Expression Omnibus (GEO) database (http://www.ncbi.nlm.nih.gov/geo), GSE144715.

2.4 Real-time PCR

The quantitative real-time polymerase chain reaction (qRT-PCR) was used for the messenger RNA (mRNA) expression assay. Total RNA was extracted from cells using the RNeasy® Plus Mini kit (Redwood City, USA). The qRT-PCR was performed using TB Green™ Premix Ex Taq™ II kit (TaKaRa, Japan). The specific primers were synthesized by Sangon Biotech Co., Ltd. (Shanghai, China). *PHLDA1*-forward: 5'-GGAGAGTAGCGGCTGCAAAG-3', *PHLDA1*-reverse: 5'-CCTCGGTGAGGATGCAACAC-3'. Biosystems™ 7500 Fast Dx Real-Time PCR system (Thermo Fisher Scientific) was used for the PCR reaction. Applied Biosystems™ 7500 Fast Real-Time PCR software (Thermo Fisher Scientific) was employed for quantitative analysis. Relative quantification was analyzed by the $2^{-\Delta\Delta C_T}$ method. *β-Actin* was used as housekeeping control.

2.5 Western blot assay

The protein expression was detected by western blot. Extracted protein from cells was quantified by BCA Protein Assay kit (Thermo Fisher Scientific), mixed with 5× sodium dodecyl sulphate-polyacrylamide gel electrophoresis (SDS-PAGE) sample loading buffer (Beyotime Biotechnology, Shanghai, China), boiled, separated by 12% (0.12 g/mL) SDS-PAGE (80 V in the stacking gel and 120 V in the separating gel), and transferred to a polyvinylidene fluoride (PVDF) membrane at 200 mA (Millipore, Billerica, MA, USA). The PVDF membrane was then blocked with 5% (0.05 g/mL) skimmed milk/phosphate-buffered saline with Tween 20 (PBST) for 60 min at room temperature, and incubated with rabbit monoclonal for PHLDA1 (Abcom, Shanghai, China) or β-actin (CST, Danvers, MA, USA) at 4 °C overnight, followed by being incubated in 5% (0.05 g/mL) skimmed milk/PBST containing anti-rabbit peroxidase-conjugated secondary antibodies (Proteintech, Wuhan, China) for 60 min at room temperature. Finally, the membranes were washed with PBST. The images of the western blot were acquired using Image Lab 3.0 by Bio-Rad ChemiDoc System (Bio-Rad, Hercules, California, USA).

2.6 Protein interaction analysis

The STRING database was used for protein–protein interaction analysis (http://string-db.org).

2.7 Statistical analysis

The continuous data were expressed as mean± standard deviation (SD). Statistical analysis between means was determined using the Student's *t*-test. *P* value of <0.05 was considered statistically significant.

3 Results

3.1 Reliability and repeatability analyses of microarray-based hypoxia/re-oxygenation-induced HUVEC transcriptome profiling

HUVECs were employed to construct hypoxia/re-oxygenation-induced VEC transcriptome profiling using an Agilent SurePrint G3 Human Gene Expression v3 Microarray. HUVECs incubated under 5% O_2, 5% CO_2, and 90% N_2 for 3 h followed by 95% air and 5% CO_2 for 1 h were used as the hypoxia/re-oxygenation group. HUVECs incubated under 95% air and 5% CO_2 were used as the normoxia control group. Rigorous data analysis was applied to ensure that genes identified

by microarray analysis were truly differentially expressed. After exclusion of absent calls and probes that were expressed in fewer than half of experimental samples, 29986 out of an initial 58339 probes (51.4%) were considered for analysis (Fig. 1a). Principal component analysis (PCA) was used to evaluate the distribution of samples in the hypoxia/re-oxygenation and normoxic control groups. The results showed that the biological repeatability and uniformity of the experimental samples were both high, which means that the experimental design was reasonable (Fig. 1b).

3.2 Hypoxia/re-oxygenation-related differentially expressed gene probes

In this study, a statistically significant up-regulation or down-regulation of differentially expressed genes was screened according to fold change of ≥2.0 and *P* value of ≤0.05. This is represented by a volcano plot (Fig. 2a). A total of 372 differentially expressed gene probes, including 106 up-regulated and 266 down-regulated gene probes, were identified. These differentially expressed gene probes were represented by a heat map of a hierarchical clustering based on HUVEC O_2 condition (Fig. 2b); the figure demonstrates very low inter-sample variation in gene expression between replicates. The top 30 differentially expressed gene probes with Entrez Gene ID that are most strongly up-regulated and down-regulated following exposure to hypoxia/re-oxygenation are listed in Tables 1 and 2. The full list of differentially regulated gene probes is shown in Table S1 and is available at http://www.ncbi.nlm.nih.gov/geo (GSE144715).

3.3 Pathways and functions mapping with hypoxia/re-oxygenation-sensitive gene probes

In order to better understand the genomic response to hypoxia/re-oxygenation of HUVECs, the 372 differentially expressed gene probes were functionally annotated and clustered using GO analysis and KEGG analysis. A total of 803 GO IDs were matched, of which 486 GO IDs were related to a biological process, 149 GO IDs were related to a cellular component, and 168 GO IDs were related to molecular function. Based on the GO analysis results, the molecular and cellular functions related to production of oxygen free radicals, calcium overload, excessive activation of inflammation, and cell injury, including endothelial cell proliferation, apoptosis, angiogenesis, vasoconstriction, and coagulation are listed in Table 3.

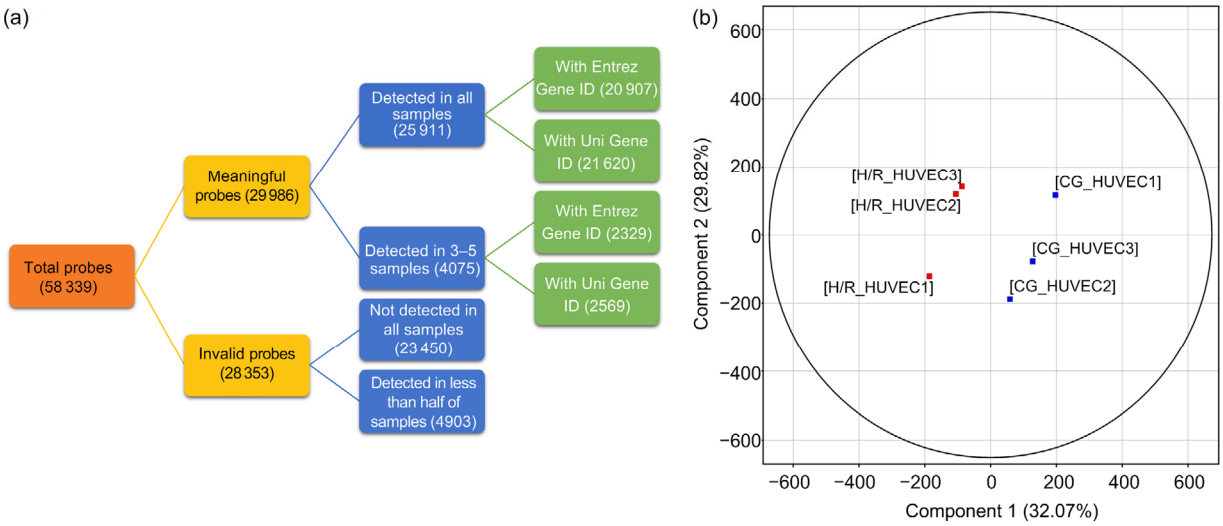

Fig. 1 Characteristics of microarray-based HUVEC hypoxia/re-oxygenation expression profile

(a) Composition analysis of microarray-based HUVEC hypoxia/re-oxygenation expression profile. A total of 58339 probes were used for microarray; 28353 probes, which were not detected in more than half of samples, were invalid probes (48.6%); 29986 probes, which were detected in more than three samples, were used for transcriptome profiling analysis (51.4%). (b) Principal component analysis (PCA). The closer the samples of the same group were in the two-dimensional space, the more representative these samples are and the better the biological repetition was. HUVEC: human umbilical vein endothelial cell; H/R_HUVEC: hypoxia/re-oxygenated group; CG_HUVEC: normoxia control group

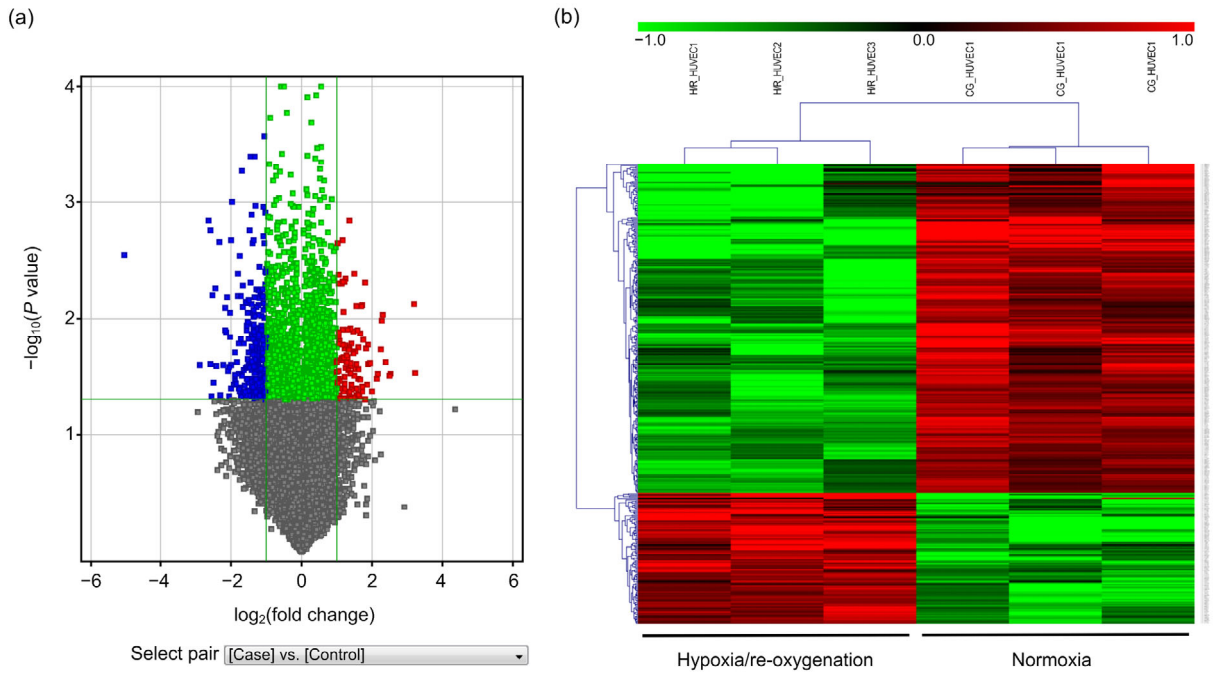

Fig. 2 Hypoxia/re-oxygenation-induced differentially regulated probes

(a) Volcano plot for differential expression screening. To analyze the significantly differently expressed genes between samples in the hypoxia/re-oxygenated and normoxia groups using the *t*-test, the $\log_2$ value of fold change is used as the abscissa, and the negative $\log_{10}$ value of the *P* value of the *t*-test is used as the ordinate to obtain the volcano plot. Gray dots: genes with the *P* value of >0.05; Green dots: genes with absolute fold change of <2 and *P* value of ≤0.05; Red dots: genes with fold change of ≥2 and *P* value ≤0.05; These are significantly up-regulated differentially expressed genes. Blue dots: genes with fold change of ≤−2 and *P* value of ≤0.05; These are significantly down-regulated differentially expressed genes. (b) Heat map of a hierarchical clustering based on HUVEC O_2 condition. Gene expression profiling of hypoxia/re-oxygenation and normoxia HUVECs demonstrated that a total of 372 probes were differentially expressed (fold change of <2, *P* value of ≤0.05). A heat map is generated where each row representes one probe set and each column representes one experimental sample. The probes are ordered by correlation and significance. The intensity of color in a cell represents the normalized expression of the probe, where red and green colorings depict high and low expression, respectively, in the hypoxia/re-oxygenation condition compared to the normoxia control

A total of 86 KEGG IDs were matched based on the known information, in which 42 differentially expressed genes were involved. Eleven differentially expressed genes participate in no less than five KEGG pathways, including fibroblast growth factor receptor 2 (*FGFR2*; 10 KEGG pathways), Wiskott-Aldrich syndrome (*WAS*; 10 KEGG pathways), aldehyde dehydrogenase 3 family, member A1 (*ALDH3A1*; 9 KEGG pathways), integrin α9 (*ITGA9*; 8 KEGG pathways), cytochrome *c* oxidase subunit VIb polypeptide 2 (testis) (*COX6B2*; 7 KEGG pathways), complement component 1, q subcomponent, A chain (*C1QA*; 6 KEGG pathways), chemokine (C-C motif) ligand 3-like 3 (*CCL3L3*; 6 KEGG pathways), chemokine (C-C motif) ligand 4-like 2 (*CCL4L2*; 6 KEGG pathways), carboxyl ester lipase (*CEL*; 5 KEGG pathways), chemokine (C-X-C motif) receptor 4 (*CXCR4*; 7 KEGG pathways), and von Willebrand factor (*VWF*; 5 KEGG pathways). Among these functionally active differentially expressed genes, *VWF* is an important endothelial cell injury marker. *CCL3L3*, *CCL4L2*, *CXCR4*, and *WAS* all participate in the chemokine signaling pathway. Therefore, we showed these two annotated KEGG pathway maps, path: hsa04610 and path:hsa04062, to indicate that these differentially expressed genes may play important roles in hypoxia/re-oxygenation, especially in inflammatory response, endothelial cytoskeleton regulation, permeability, cellular growth and differentiation, cell lysis, apoptosis, reactive oxygen species (ROS) production, and nitric oxide (NO) production (Fig. 3).

Table 1 Thirty most highly up-regulated genes with Entrez Gene ID of HUVECs induced by hypoxia/re-oxygenation

Probe name	Gene name	Gene symbol	Gene identifier	Entrez Gene ID	Fold change*	*P* value
A_23_P21057	Septin 1	*SEPT1*	NM_052838	1731	9.36	0.03
A_32_P211248	Long intergenic non-protein coding RNA 1405	*LINC01405*	NR_036513	100131138	9.23	0.01
A_21_P0012449	Long intergenic non-protein coding RNA 971	*LINC00971*	NR_033860	440970	5.77	0.03
A_21_P0000019	Lysine demethylase 4C	*KDM4C*	NM_001146695	23081	5.70	0.03
A_24_P366122	Acyl-CoA binding domain containing 4	*ACBD4*	NM_024722	79777	4.95	0.01
A_24_P160380	PDZ and LIM domain 2	*PDLIM2*	NM_176871	64236	4.84	0.01
A_22_P00002166	Family with sequence similarity 229, member A	*FAM229A*	NM_001167676	100128071	4.39	0.03
A_33_P3285271	Flavin containing dimethylaniline monooxygenase 6 pseudogene	*FMO6P*	NR_002601	388714	3.88	0.02
A_33_P3422085	SPANX family member N2	*SPANXN2*	NM_001009615	494119	3.73	0.02
A_23_P159893	Chordin-like 1	*CHRDL1*	NM_145234	91851	3.64	0.04
A_22_P00014410	SACS antisense RNA 1	*SACS-AS1*	NR_103450	100506680	3.51	0.05
A_33_P3423425	Zinc finger protein 770	*ZNF770*	NM_014106	54989	3.49	0.00
A_24_P322229	RAS like family 10 member B	*RASL10B*	NM_033315	91608	3.39	0.02
A_33_P3211078	High mobility group AT-hook 2	*HMGA2*	NM_001300918	8091	3.33	0.04
A_21_P0001900	Gastric cancer associated transcript 1	*GACAT1*	NR_126369	104326057	3.22	0.01
A_33_P3384710	Family with sequence similarity 222 member B	*FAM222B*	NM_001288631	55731	3.19	0.01
A_23_P420692	Protein tyrosine phosphatase receptor type F (PTPRF) interacting protein α 4	*PPFIA4*	XM_006711588	8497	3.04	0.02
A_33_P3286953	ADAM metallopeptidase with thrombospondin type 1 motif 6	*ADAMTS6*	NM_197941	11174	2.96	0.02
A_23_P102000	C-X-C motif chemokine receptor 4	*CXCR4*	NM_001008540	7852	2.95	0.05
A_33_P3294302	Pleckstrin homology-like domain family A member 1	*PHLDA1*	NM_007350	22822	2.87	0.02
A_21_P0006019	Uncharacterized LOC101927358	*LOC101927358*	NR_121182	101927358	2.84	0.03
A_22_P00009701	Uncharacterized LOC100131655	*LOC100131655*	NR_040024	100131655	2.81	0.05
A_24_P362904	6-Phosphofructo-2-kinase/fructose-2,6-biphosphatase 4	*PFKFB4*	NM_004567	5210	2.81	0.05
A_33_P3771067	Uncharacterized LOC283140	*LOC283140*	NR_126004	283140	2.79	0.02
A_23_P46131	Family with sequence similarity 110 member D	*FAM110D*	NM_024869	79927	2.67	0.04
A_23_P45751	Chloride channel accessory 4	*CLCA4*	NM_012128	22802	2.66	0.02
A_23_P16415	Low density lipoprotein (LDL) receptor-related protein 3	*LRP3*	NM_002333	4037	2.66	0.04
A_23_P62647	Signaling lymphocytic activation molecule family member 1	*SLAMF1*	NM_003037	6504	2.64	0.02
A_24_P221575	RUN and FYVE domain containing 3	*RUFY3*	NM_001037442	22902	2.63	0.03
A_33_P3222018	Chromobox 3	*CBX3*	NM_007276	11335	2.62	0.03

* The fold change is (hypoxia/re-oxygenation group)/(normoxia group)

Table 2 Thirty most highly down-regulated genes with Entrez Gene ID of HUVECs induced by hypoxia/re-oxygenation

Probe name	Gene name	Gene symbol	Gene identifier	Entrez Gene ID	Fold change*	*P* value
A_21_P0007488	Long intergenic non-protein coding RNA 1490	*LINC01490*	NR_120468	101928420	33.12	0.00
A_22_P00018708	Uncharacterized LOC101927913	*LOC101927913*	XR_241962	101927913	7.43	0.03
A_23_P389500	Regenerating family member 1 β	*REG1B*	NM_006507	5968	6.02	0.00
A_22_P00020802	Uncharacterized LOC101927694	*LOC101927694*	NR_104648	101927694	5.67	0.04
A_33_P3268035	Lysozyme-like 1	*LYZL1*	NM_032517	84569	5.35	0.03
A_24_P327084	Serine protease 33	*PRSS33*	NM_152891	260429	5.02	0.00
A_23_P86411	Myosin IIIA	*MYO3A*	NM_017433	53904	4.47	0.01
A_23_P111978	Potassium two-pore-domain channel subfamily K member 9	*KCNK9*	NM_001282534	51305	4.46	0.01
A_21_P0009060	Uncharacterized LOC101928035	*LOC101928035*	NR_104657	101928035	4.31	0.01
A_23_P36050	Olfactory receptor family 8 subfamily K member 3 (gene/pseudogene)	*OR8K3*	NM_001005202	219473	4.26	0.03
A_23_P502590	Killer cell immunoglobulin-like receptor, two Ig domains and short cytoplasmic tail 4	*KIR2DS4*	NM_012314	3809	4.17	0.05
A_33_P3238182	Long intergenic non-protein coding RNA 588	*LINC00588*	NR_026772	26138	4.14	0.03
A_19_P00809368	Long intergenic non-protein coding RNA 1215	*LINC01215*	NR_110028	101929623	4.06	0.01
A_32_P234926	BANF family member 2	*BANF2*	NM_001014977	140836	4.04	0.04
A_32_P155666	Endothelin converting enzyme-like 1	*ECEL1*	NM_004826	9427	4.03	0.00
A_21_P0001945	Uncharacterized LOC101927156	*LOC101927156*		101927156	4.00	0.03
A_24_P361427	TBC1 domain family member 29	*TBC1D29*	NM_015594	26083	3.76	0.04
A_22_P00010840	Uncharacterized LOC101927272	*LOC101927272*	NR_110908	101927272	3.74	0.02
A_21_P0010721	Long intergenic non-protein coding RNA 869	*LINC00869*	XR_426752	57234	3.62	0.04
A_23_P419156	Opsin 1, short wave sensitive	*OPN1SW*	NM_001708	611	3.55	0.02
A_22_P00014526	CFAP44 antisense RNA 1	*CFAP44-AS1*	NR_046728	100874029	3.49	0.01
A_21_P0004097	Uncharacterized LOC101929261	*LOC101929261*	XR_241733	101929261	3.47	0.02
A_33_P3235721	Chromosome 11 open reading frame 87	*C11orf87*	NM_207645	399947	3.42	0.04
A_22_P00002954	Uncharacterized LOC101929261	*LOC101929261*	XR_241733	101929261	3.38	0.04
A_33_P3882624	Protection of telomeres 1	*POT1*	NM_015450	25913	3.36	0.00
A_33_P3262635	Cat eye syndrome chromosome region, candidate 1	*CECR1*	NM_001282225	51816	3.30	0.05
A_21_P0004219	Long intergenic non-protein coding RNA 1018	*LINC01018*	NR_024424	255167	3.30	0.01
A_33_P3307795	Family with sequence similarity 124 member B	*FAM124B*	NM_024785	79843	3.28	0.00
A_22_P00008580	Long intergenic non-protein coding RNA 1231	*LINC01231*	NR_121585	101929247	3.26	0.03
A_23_P150064	Multimerin 2	*MMRN2*	NM_024756	79812	3.19	0.04

* The fold change is (normoxia group)/(hypoxia/re-oxygenation group)

Table 3 Pathways and functions associated with hypoxia/re-oxygenation analyzed by GO

Hypoxia/re-oxygenation-related GO	GO ID	Related differentially regulated gene	Fold enrichment[#]	*P* value[*]
Production of oxygen free radicals				
Positive regulation of phospholipase activity	GO:0010518	*FGFR2*	22.13	0.05
Negative regulation of nitric-oxide synthase activity	GO:0051001	*CNR2*	22.13	0.05
Neutrophil activation	GO:0042119	*CXCR4*	17.70	0.06
Nitric-oxide synthase binding	GO:0050998	*SCN5A*	11.94	0.09
Dioxygenase activity	GO:0051213	*KDM4C*	9.83	0.10
Response to hypoxia	GO:0001666	*CXCR4*, *ALDH3A1*	2.23	0.23
Calcium overload				
G-protein-coupled receptor signaling pathway	GO:0007186	*GPR31*, *OPN1SW*, *OR13H1*, *OR2A2*, *NPBWR1*, *NPY6R*, *OR10G8*, *OR10J3*, *OR8K3*, *CCL3L3*, *CXCR4*, *ADGRG3*, *OR10J5*, *FFAR2*	3.11	0.00
Sodium ion transmembrane transport	GO:0035725	*SLC5A5*, *ASIC2*, *SCN5A*	6.43	0.01
Lipid digestion	GO:0044241	*CEL*	29.51	0.04
Sodium ion transport	GO:0006814	*SLC38A3*, *SCN5A*	4.82	0.07
Phospholipase binding	GO:0043274	*WAS*	9.28	0.11
Calcium channel regulator activity	GO:0005246	*NPY*	5.96	0.16
Phosphatidylinositol phospholipase C activity	GO:0004435	*PLCH2*	5.96	0.16
Excessive activation of inflammation				
Negative regulation of interferon-γ biosynthetic process	GO:0045077	*INHA*	35.42	0.03
Neutrophil chemotaxis	GO:0030593	*ITGA9*, *CCL3L3*	5.57	0.05
Chemokine-mediated signaling pathway	GO:0070098	*CCL3L3*, *CXCR4*	5.09	0.06
Complement activation	GO:0006956	*C1QA*	3.68	0.24
Positive regulation of inflammatory response	GO:0050729	*CCL3L3*	3.10	0.28
Cell injury				
Regulation of vascular endothelial growth factor receptor signaling pathway	GO:0030947	*TMEM204*	35.42	0.03
Positive regulation of epithelial cell proliferation	GO:0050679	*FGFR2*, *SCN5A*	6.05	0.05
Negative regulation of cell migration involved in sprouting angiogenesis	GO:0090051	*MMRN2*	22.13	0.05
Blood coagulation, intrinsic pathway	GO:0007597	*VWF*	9.83	0.10
Positive regulation of cell proliferation	GO:0008284	*SLAMF1*, *VWCE*, *FGFR2*, *KDM4C*, *ALDH3A1*	2.03	0.11
Regulation of vasoconstriction	GO:0019229	*ASIC2*	8.42	0.12
Angiogenesis	GO:0001525	*MMRN2*, *FGFR2*, *NRCAM*	2.47	0.13
Positive regulation of apoptotic process	GO:0043065	*PHLDA1*, *HMGA2*, *NEURL1*	1.89	0.22
DNA damage response, signal transduction by p53 class mediator resulting in cell cycle arrest	GO:0006977	*PSMB11*	2.67	0.32
Apoptotic process	GO:0006915	*PSMB11*, *PHLDA1*, *FGFR2*, *CXCR4*	1.17	0.45
Negative regulation of cell proliferation	GO:0008285	*CCL3L3*, *NEURL1*	0.92	0.64

[#] Fold enrichmen=(list hits/list total)/(population hits/population total), where "list hits" is the number of differentially expressed genes annotated to each Gene Ontology (GO)/Kyoto Encyclopedia of Genes and Genomes (KEGG) entry, "list total" is the number of differentially expressed genes involved in GO/KEGG analysis, "population hits" is the number of genes in whole microarray annotated to each GO/KEGG entry, and "population total" is the number of genes in whole microarray involved in GO/KEGG analysis. [*] *P* value of fold enrichment, and $P \leq 0.05$ indicates significant enrichment

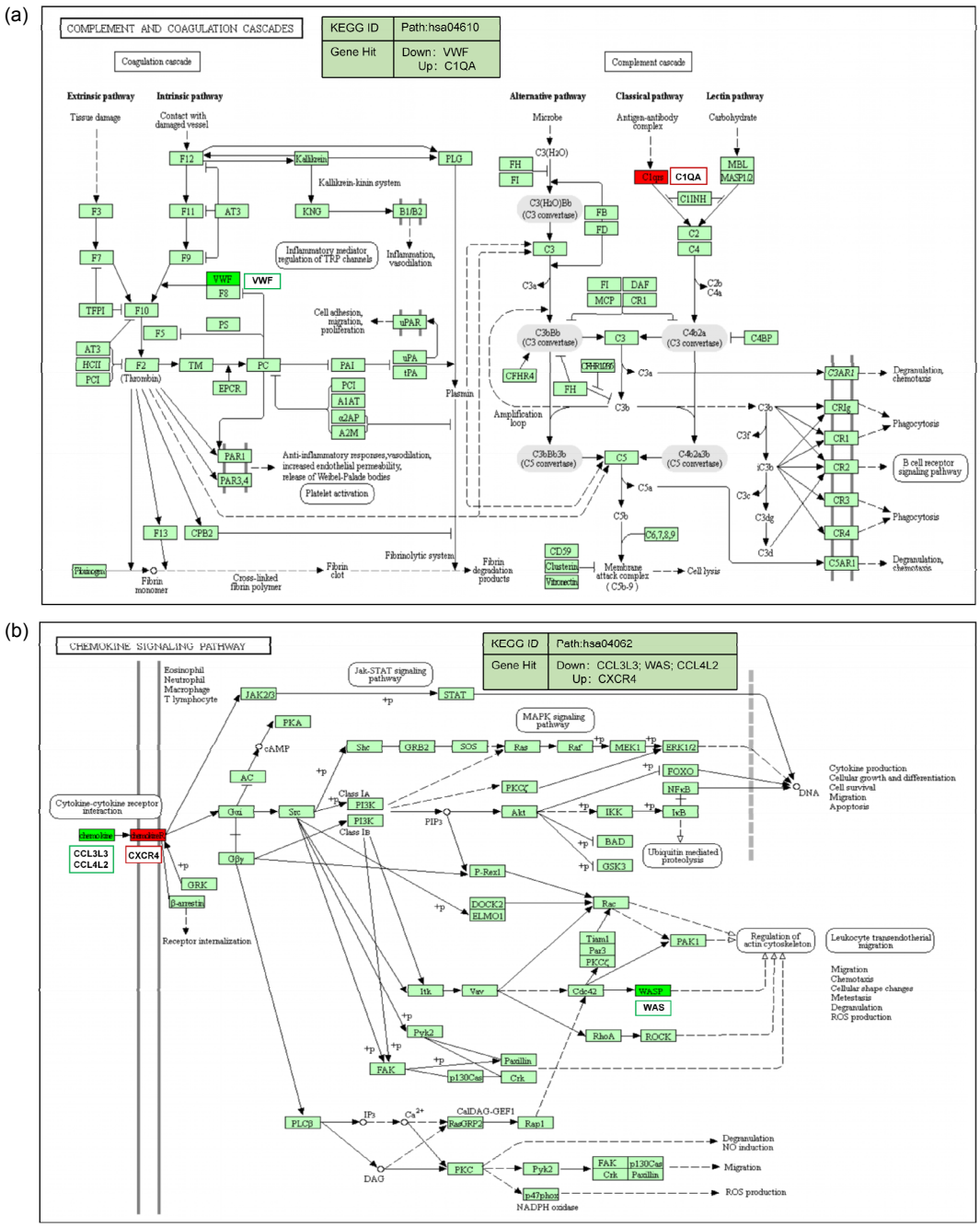

Fig. 3 Hypoxia/re-oxygenation-related KEGG pathway and differentially expressed genes

(a) von Willebrand factor (*VWF*), complement component 1, q subcomponent, A chain (*C1QA*), and complement and coagulation cascades pathway. On the map of the complement and coagulation cascades pathway, endothelial cell injury marker *VWF*, which is significantly down-expressed in hypoxia/re-oxygenation group in our database, plays an important role in thrombogenesis, endothelial permeability, and anti-inflammatory responses. *C1QA*, which is significantly up-expressed in the hypoxia/re-oxygenation group in our database, initiates the complement cascade and is involved in cell lysis, chemotaxis, and phagocytosis. The migration, aggregation, and phagocytosis of neutrophils are the important mechanisms leading to the large release of reactive oxygen species (ROS) during ischemia-reperfusion injury. (b) Chemokine (C-C motif) ligand 3-like 3 (*CCL3L3*), chemokine (C-C motif) ligand 4-like 2 (*CCL4L2*), chemokine (C-X-C motif) receptor 4 (*CXCR4*), Wiskott-Aldrich syndrome (*WAS*), and chemokine signaling pathway. Significantly down-expressed chemokines *CCL3L3* and *CCL4L2* and significantly up-expressed chemokine receptor *CXCR4* are the initiating molecules of the chemokine signaling pathway. This pathway is crucial in cellular growth and differentiation, cell survival and apoptosis, ROS and nitric oxide (NO) production. *WAS*, which is on one branch involved in regulation of actin cytoskeleton, is significantly down-expressed in the hypoxia/re-oxygenation group in our database

3.4 Expression verification of differentially expressed gene *PHLDA1* and exploration of related function based on HUVEC hypoxia/re-oxygenation transcriptome profiling

PHLDA1 was first identified as a potential transcription factor required for Fas expression and activation-induced apoptosis in mouse T cell hybridomas (Moad et al., 2013). However, its expression is induced by a variety of external stimuli, and it participates in apoptosis, autophagy, cell proliferation and differentiation, inflammation, and fat metabolism (Johnson et al., 2011; Sellheyer and Nelson, 2011). Recently, PHLDA1 has received increased attention because of its association with cancer (Nagai, 2016; Fearon et al., 2018). In our microarray database, *PHLDA1* was significantly up-expressed in the hypoxia/re-oxygenation group. Using real-time PCR and western blot assay, we validated that the mRNA and protein were both significantly highly expressed in the hypoxia/re-oxygenation group compared to the normoxia group (Figs. 4a–4c). Based on the STRING search results of PHLDA1 protein–protein interactions (Fig. 4d), we found many potentially related proteins SLC38A3, SLC5A5, Lnc-SLC36A4-1, and Lnc-PLEKHJ1-1 in our differentially expressed database.

4 Discussion

The known VEC hypoxia/re-oxygenation injury mechanisms consist of a complex pathophysiology involving activation of cell death programs, endothelial dysfunction, transcriptional reprogramming, and activation of the innate and adaptive immune system. Numerous pathways and signaling cascades are implicated (Salvadori et al., 2015). VECs undergo swelling, loss of pinocytotic vesicles, degradation of the cytoskeleton, and lifting from the underlying basement

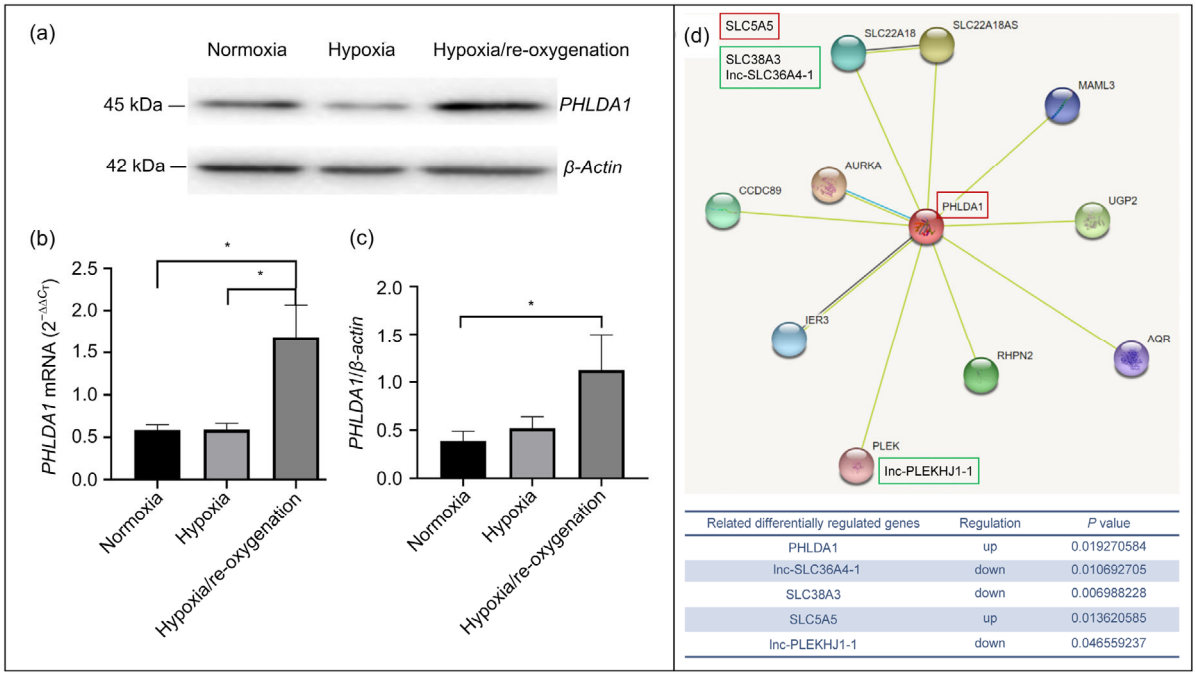

Related differentially regulated genes	Regulation	*P* value
PHLDA1	up	0.019270584
lnc-SLC36A4-1	down	0.010692705
SLC38A3	down	0.006988228
SLC5A5	up	0.013620585
lnc-PLEKHJ1-1	down	0.046559237

Fig. 4 Expression verification of differentially expressed gene *PHLDA1* and exploration of function-related genes based on HUVEC microarray database

(a, c) Western blot measurement of *PHLDA1* expression in HUVECs influenced by hypoxia/re-oxygenation. (b) Effects of hypoxia/re-oxygenation on the mRNA expression of *PHLDA1* in HUVECs. Results are normalized to *β-actin*. Data are expressed as mean±standard deviation (SD), n=3. Normoxia group: HUVECs incubated under 95% air and 5% CO_2; Hypoxia group: HUVECs incubated under 5% O_2, 5% CO_2 and 90% N_2 for 3 h; Hypoxia/re-oxygenation group: HUVECs incubated under hypoxia for 3 h followed by 95% air and 5% CO_2 for 1 h. * P<0.05, compared with the hypoxia/re-oxygenation group. (d) PHLDA1-related protein–protein interaction analysis using STRING database. The interactions include both the direct physical interactions between proteins and the indirect functional correlations between proteins. Related proteins SLC38A3, SLC5A5, Lnc-SLC36A4-1, and Lnc-PLEKHJ1-1 were significantly differentially expressed in our database

membrane. As a consequence, intercellular contact of endothelial cells is lost, increasing vascular permeability and fluid loss to the interstitial space (Basile et al., 2011). In addition, there is impaired endothelial function by directly reducing endothelial NO production at the transcriptional and posttranscriptional levels, leading to vasoconstriction and aggravating tissue ischemia despite reperfusion (McQuillan et al., 1994; Liao et al., 1995). Another important feature of VEC hypoxia/re-oxygenation injury is the chemotaxis of leukocytes, the accumulation and adhesion of circulating leukocytes (primarily neutrophils) to the endothelial cell surface, and enhanced oxidative stress, leading to vessel inflammation and progression (Eltzschig and Collard, 2004). As shown by research, this process is initiated by increased expression of P-selectin on the VECs and interaction of P-selectin with P-selectin glycoprotein 1 (PSGL-1) expressed on the leukocytes. Subsequently, firm adherence of the leucocytes to the endothelium is achieved by the interaction of the β2-integrins lymphocyte function-associated antigen I (LFA-I) and macrophage-l antigen (MAC-I or complement receptor 3 (CR3)) on the leukocyte and the intracellular adhesion molecule 1 (ICAM-I) on the VEC. Platelet endothelial cell adhesion molecule 1 (PECAM-I) facilitates leukocyte transmigration into the interstitial space (Carden and Granger, 2000).

The present study used whole-transcriptome microarray to explore the genomic response of HUVECs to hypoxia/re-oxygenation. The microarray analysis identified that approximately 29986 gene probes were involved in regulation under hypoxia/re-oxygenation exposure. Among them, 106 up-regulated gene probes and 266 down-regulated gene probes were identified as the differentially expressed gene probes. These encompass gene probes were involved in a multitude of pathways and functions, including production of oxygen free radicals, calcium overload, excessive activation of inflammation, glucose and lipid metabolism, endothelial cell proliferation, differentiation, cytoskeleton regulation, permeability, cell lysis, apoptosis, and angiogenesis. Many of the aforementioned VEC hypoxia/re-oxygenation-related genes (such as: regulation of actin cytoskeleton-related *WAS*; NO synthase-related *CNR2*, *SCN5A*; regulation of vasoconstriction-related *ASIC2*; neutrophil chemotaxis and adhesion-related *CCL3L3*, *CCL4L2*, *CXCR4*, *ITGA9*; neutrophil activation and ROS-related *CXCR4*, *KDM4C*; regulation of cell proliferation and apoptosis-related *SLAMF1*, *VWCE*, *FGFR2*, *KDM4C*, *ALDH3A1*, *NEURL*, *PHLDA1*, *HMGA2*, *PSMB11*) were all found differentially expressed in the hypoxia/re-oxygenation group in our database. However, many VECs functionally related important genes (such as: the endothelial cell injury marker and coagulation-related *VWF*; regulation of vascular endothelial growth factor (VEGF) receptor signaling pathway-related *TMEM204*; angiogenesis-related *MMRN2*, *FGFR2*, *NRCAM*) and ischaemia and reperfusion injury (IRI)-related genes (such as: phosphatidylinositol phospholipase C (PLC) activity-related *PLCH2*; ion transport-related *SLC38A3*, *SCN5A*, *NPY*; complement activation-related *C1QA*; lipid digestion-related *CEL*), which were found as the differentially expressed genes, may also play a crucial role in VEC hypoxia/re-oxygenation injury.

In fact, many meaningful hypoxia genes, such as hypoxia-inducible factor 1-α (*HIF1A*) and VEGF-related genes, were also contained in the microarray, including probes A_24_P56388 (*HIF1A*), A_33_P3231277 (*HIF1A*), A_22_P00016429 (HIF1A antisense RNA 1 (*HIF1A-AS1*)), A_22_P00020043 (*HIF1A-AS1*), A_23_P46964 (*HIF1AN*), A_33_P3338152 (*HIF3A*), A_23_P142187 (*HIF3A*), A_23_P338534 (*HIF3A*), A_24_P12401 (*VEGFA*), A_23_P70398 (*VEGFA*), A_23_P1594 (*VEGFB*), A_23_P167096 (*VEGFC*), and A_21_P0003801 (*Lnc-VEGFC-1*). However, the expression levels of these genes were not significantly different between the hypoxic/re-oxygenated group and the normoxia group. On the one hand, it may be because these genes are indeed not significantly different in this model; on the other hand, it may be because they are more active under the condition of hypoxia and are relatively silent after re-oxygenation, while other genes are more active.

In addition, it has been found that endothelial cells are particularly resistant to hypoxic stress, and can maintain proliferation even after having been cultured in mild hypoxia in a time-dependent manner (Bader et al., 2015; Sun et al., 2015; Baldea et al., 2018). Our results are also consistent with the above research. As mentioned earlier, PHLDA1 acts as a mediator of apoptosis (Moad et al., 2013), plays an important role in cancer (Nagai, 2016), and is annotated to "positive regulation of the apoptotic process" GO ID (Table 3). Expression verification of PHLDA1

mRNA or protein in our study had no obvious change after only exposure to hypoxia for 3 h (5% O_2), but was significantly up-expressed after re-oxygenation. This is consistent with our microarray results (Fig. 4). Recent research has also shown that PHLDA1 was highly expressed in myocardial ischemia-reperfusion injuries, and knockdown of PHLDA1 can attenuate oxidative stress-induced ROS production and apoptosis in cardiomyocytes (Guo et al., 2020). PHLDA1 may promote oxidative stress-related apoptosis by binding to BCL2-associated X, apoptosis regulator (BAX). This research further validates our research in which PHLDA1 may play an important role in VEC hypoxia/re-oxygenation injury.

Long non-coding RNAs (lncRNAs) in the nucleus have functions in histone modification and block the binding of transcription factors to their promoters or direct transcriptional regulation (E et al., 2018; Mansoori et al., 2018). More than 200 diseases are related to dysregulated or dysfunctional lncRNAs (Zampetaki et al., 2018; Fu et al., 2019; Gudenas et al., 2019). Thus, exploration and identification of hypoxia/re-oxygenation-associated lncRNAs and their functions may provide a new insight into the understanding of VEC hypoxia/re-oxygenation pathogenesis and define novel therapeutic targets. Recent research reported that lncRNA *HIF1A-AS2* can recruit lysine-specific demethylase 1 (LSD1) and epigenetically repress *PHLDA1* (Mineo et al., 2016). STRING analysis results showed that significantly differentially expressed genes *SLC38A3*, *SLC5A5*, *Lnc-SLC36A4-1*, and *Lnc-PLEKHJ1-1* in our database may have physical or/and functional protein–protein interactions with *PHLDA1* (Fig. 4d). The interconnectedness of these genes is expected to reveal some potential hypoxia/re-oxygenation mechanisms related to lncRNAs. However, the validation of PHLDA1 and the analysis of interacting proteins were just one of many new discoveries in this study, and more validation and mechanism studies of the hypoxia/re-oxygenation genes found here will be further revealed.

5 Conclusions

In summary, our microarray-based HUVEC hypoxia/re-oxygenation transcriptome profiling research was reasonable in design, with high reliability and repeatability. The differentially expressed genes revealed by the microarray largely compensate for the existing VEC hypoxia/re-oxygenation-related databases. Through GO, KEGG, and STRING analyses, we explored the new VEC hypoxia/re-oxygenation-related functions and protein–protein interactions, and put forward hypotheses for possible mechanisms of some lncRNAs. We believe that the results of this study have significance for understanding the mechanism of VEC hypoxia/re-oxygenation injury.

Contributors

Jia XU performed the experimental research and data analysis, wrote and edited the manuscript. Jiu-kun JIANG performed the establishment of models. Xiao-lin LI, Xiao-peng YU, and Ying-ge XU conducted molecular biology experiments. Yuan-qiang LU performed the study design, data analysis, writing and editing of the manuscript. All authors have read and approved the final manuscript and, therefore, have full access to all the data in the study and take responsibility for the integrity and security of the data.

Compliance with ethics guidelines

Jia XU, Jiu-kun JIANG, Xiao-lin LI, Xiao-peng YU, Ying-ge XU, and Yuan-qiang LU declare that they have no conflict of interest.

This article does not contain any studies with human or animal subjects performed by any of the authors.

References

Atkeson A, Yeh SY, Malhotra A, et al., 2009. Endothelial function in obstructive sleep apnea. *Prog Cardiovasc Dis*, 51(5):351-362. https://doi.org/10.1016/j.pcad.2008.08.002

Bader AM, Klose K, Bieback K, et al., 2015. Hypoxic preconditioning increases survival and pro-angiogenic capacity of human cord blood mesenchymal stromal cells *in vitro*. *PLoS ONE*, 10(9):e0138477. https://doi.org/10.1371/journal.pone.0138477

Baldea I, Teacoe I, Olteanu DE, et al., 2018. Effects of different hypoxia degrees on endothelial cell cultures—time course study. *Mech Ageing Dev*, 172:45-50. https://doi.org/10.1016/j.mad.2017.11.003

Basile DP, Friedrich JL, Spahic J, et al., 2011. Impaired endothelial proliferation and mesenchymal transition contribute to vascular rarefaction following acute kidney injury. *Am J Physiol Renal Physiol*, 300(3):F721-F733. https://doi.org/10.1152/ajprenal.00546.2010

Carden DL, Granger DN, 2000. Pathophysiology of ischaemia-reperfusion injury. *J Pathol*, 190(3):255-266. https://doi.org/10.1002/(SICI)1096-9896(200002)190:3<255::AID-PATH526>3.0.CO;2-6

E S, Costa MC, Kurc S, et al., 2018. The circulating non-coding RNA landscape for biomarker research: lessons

and prospects from cardiovascular diseases. *Acta Pharmacol Sin*, 39(7):1085-1099. https://doi.org/10.1038/aps.2018.35

Eltzschig HK, Collard CD, 2004. Vascular ischaemia and reperfusion injury. *Br Med Bull*, 70(1):71-86. https://doi.org/10.1093/bmb/ldh025

Fearon AE, Carter EP, Clayton NS, et al., 2018. PHLDA1 mediates drug resistance in receptor tyrosine kinase-driven cancer. *Cell Rep*, 22(9):2469-2481. https://doi.org/10.1016/j.celrep.2018.02.028

Ferrucci M, Biagioni F, Ryskalin L, et al., 2018. Ambiguous effects of autophagy activation following hypoperfusion/ischemia. *Int J Mol Sci*, 19(9):2756. https://doi.org/10.3390/ijms19092756

Filippi I, Saltarella I, Aldinucci C, et al., 2018. Different adaptive responses to hypoxia in normal and multiple myeloma endothelial cells. *Cell Physiol Biochem*, 46(1):203-212. https://doi.org/10.1159/000488423

Fu PF, Zheng X, Fan X, et al., 2019. Role of cytoplasmic lncRNAs in regulating cancer signaling pathways. *J Zhejiang Univ-Sci B (Biomed & Biotechnol)*, 20(1):1-8. https://doi.org/10.1631/jzus.B1800254

Gudenas BL, Wang J, Kuang SZ, et al., 2019. Genomic data mining for functional annotation of human long noncoding RNAs. *J Zhejiang Univ-Sci B (Biomed & Biotechnol)*, 20(6):476-487. https://doi.org/10.1631/jzus.B1900162

Guo YX, Jia PY, Chen YQ, et al., 2020. PHLDA1 is a new therapeutic target of oxidative stress and ischemia reperfusion-induced myocardial injury. *Life Sci*, 245:117347. https://doi.org/10.1016/j.lfs.2020.117347

Haybar H, Shokuhian M, Bagheri M, et al., 2019. Involvement of circulating inflammatory factors in prognosis and risk of cardiovascular disease. *J Mol Cell Cardiol*, 132:110-119. https://doi.org/10.1016/j.yjmcc.2019.05.010

Jiang JK, Fang W, Hong LJ, et al., 2017. Distribution and differentiation of myeloid-derived suppressor cells after fluid resuscitation in mice with hemorrhagic shock. *J Zhejiang Univ-Sci B (Biomed & Biotechnol)*, 18(1):48-58. https://doi.org/10.1631/jzus.B1600510

Johnson EO, Chang KH, de Pablo Y, et al., 2011. PHLDA1 is a crucial negative regulator and effector of Aurora A kinase in breast cancer. *J Cell Sci*, 124(16):2711-2722. https://doi.org/10.1242/jcs.084970

Li F, Lee KE, Simon MC, 2018. Detection of hypoxia and HIF in paraffin-embedded tumor tissues. *In*: Huang LE (Ed.), Hypoxia: Methods and Protocols. Humana Press, New York, p.277-282. https://doi.org/10.1007/978-1-4939-7665-2_24

Li WY, Zhao YL, Fu P, 2018. Hypoxia induced factor in chronic kidney disease: friend or foe? *Front Med (Lausanne)*, 4:259. https://doi.org/10.3389/fmed.2017.00259

Liao JK, Zulueta JJ, Yu FS, et al., 1995. Regulation of bovine endothelial constitutive nitric oxide synthase by oxygen. *J Clin Invest*, 96(6):2661-2666. https://doi.org/10.1172/JCI118332

Lim To WK, Kumar P, Marshall JM, 2015. Hypoxia is an effective stimulus for vesicular release of ATP from human umbilical vein endothelial cells. *Placenta*, 36(7):759-766. https://doi.org/10.1016/j.placenta.2015.04.005

Mansoori Z, Ghaedi H, Sadatamini M, et al., 2018. Down-regulation of long non-coding RNAs *LINC00523* and *LINC00994* in type 2 diabetes in an Iranian cohort. *Mol Biol Rep*, 45(5):1227-1233. https://doi.org/10.1007/s11033-018-4276-7

McQuillan LP, Leung GK, Marsden PA, et al., 1994. Hypoxia inhibits expression of eNOS via transcriptional and post-transcriptional mechanisms. *Am J Physiol*, 267(5):H1921-H1927. https://doi.org/10.1152/ajpheart.1994.267.5.H1921

Mineo M, Ricklefs F, Rooj AK, et al., 2016. The long non-coding RNA HIF1A-AS2 facilitates the maintenance of mesenchymal glioblastoma stem-like cells in hypoxic niches. *Cell Rep*, 15(11):2500-2509. https://doi.org/10.1016/j.celrep.2016.05.018

Moad AIH, Muhammad TST, Oon CE, et al., 2013. Rapamycin induces apoptosis when autophagy is inhibited in T-47D mammary cells and both processes are regulated by Phlda1. *Cell Biochem Biophys*, 66(3):567-587. https://doi.org/10.1007/s12013-012-9504-5

Nagai MA, 2016. Pleckstrin homology-like domain, family A, member 1 (PHLDA1) and cancer (Review). *Biomed Rep*, 4(3):275-281. https://doi.org/10.3892/br.2016.580

Nallamshetty S, Chan SY, Loscalzo J, 2013. Hypoxia: a master regulator of microRNA biogenesis and activity. *Free Radic Biol Med*, 64:20-30. https://doi.org/10.1016/j.freeradbiomed.2013.05.022

Niu QF, Li DL, Yang Y, et al., 2019. Establishment of human vascular endothelial hypoxia/reoxygeneration injury cell model. *China J Oral Maxillofac Surg*, 17(4):295-299 (in Chinese). https://doi.org/10.19438/j.cjoms.2019.04.002

Pan H, Wang BH, Li ZB, et al., 2019. Mitochondrial superoxide anions induced by exogenous oxidative stress determine tumor cell fate: an individual cell-based study. *J Zhejiang Univ-Sci B (Biomed & Biotechnol)*, 20(4):310-321. https://doi.org/10.1631/jzus.B1800319

Pan J, Zhu JY, Kee HS, et al., 2015. A review of compression, ventilation, defibrillation, drug treatment, and targeted temperature management in cardiopulmonary resuscitation. *Chin Med J (Engl)*, 128(4):550-554. https://doi.org/10.4103/0366-6999.151115

Salvadori M, Rosso G, Bertoni E, 2015. Update on ischemia-reperfusion injury in kidney transplantation: pathogenesis and treatment. *World J Transplant*, 5(2):52-67. https://doi.org/10.5500/wjt.v5.i2.52

Sellheyer K, Nelson P, 2011. Follicular stem cell marker PHLDA1 (TDAG51) is superior to cytokeratin-20 in differentiating between trichoepithelioma and basal cell

carcinoma in small biopsy specimens. *J Cutan Pathol*, 38(7):542-550. https://doi.org/10.1111/j.1600-0560.2011.01693.x

Shay JES, Celeste Simon M, 2012. Hypoxia-inducible factors: crosstalk between inflammation and metabolism. *Semin Cell Dev Biol*, 23(4):389-394. https://doi.org/10.1016/j.semcdb.2012.04.004

Sun Y, George J, Rocha S, 2015. Dose-dependent effects of allopurinol on human foreskin fibroblast cells and human umbilical vein endothelial cells under hypoxia. *PLoS ONE*, 10(4):e0123649. https://doi.org/10.1371/journal.pone.0123649

Tang X, Lin CP, Guo DQ, et al., 2016. CLOCK promotes endothelial damage by inducing autophagy through reactive oxygen species. *Oxid Med Cell Longev*, 2016:9591482. https://doi.org/10.1155/2016/9591482

Taylor MA, Das BC, Ray SK, 2018. Targeting autophagy for combating chemoresistance and radioresistance in glioblastoma. *Apoptosis*, 23(11-12):563-575. https://doi.org/10.1007/s10495-018-1480-9

Urbanek T, Kuczmik W, Basta-Kaim A, et al., 2014. Rapamycin induces of protective autophagy in vascular endothelial cells exposed to oxygen-glucose deprivation. *Brain Res*, 1553:1-11. https://doi.org/10.1016/j.brainres.2014.01.017

Wang JC, Li XX, Sun X, et al., 2018. Activation of AMPK by simvastatin inhibited breast tumor angiogenesis via impeding HIF-1α-induced pro-angiogenic factor. *Cancer Sci*, 109(5):1627-1637. https://doi.org/10.1111/cas.13570

Wu JB, Lei Z, Yu JG, 2015. Hypoxia induces autophagy in human vascular endothelial cells in a hypoxia-inducible factor 1-dependent manner. *Mol Med Rep*, 11(4):2677-2682. https://doi.org/10.3892/mmr.2014.3093

Xie XJ, Yang YM, Jiang JK, et al., 2017. Association between the vascular endothelial growth factor single nucleotide polymorphisms and diabetic retinopathy risk: a meta-analysis. *J Diabetes*, 9(8):738-753. https://doi.org/10.1111/1753-0407.12480

Zampetaki A, Albrecht A, Steinhofel K, 2018. Long non-coding RNA structure and function: is there a link? *Front Physiol*, 9:1201. https://doi.org/10.3389/fphys.2018.01201

Zhang Q, Fang W, Ma L, et al., 2018. VEGF levels in plasma in relation to metabolic control, inflammation, and microvascular complications in type-2 diabetes: a cohort study. *Medicine (Baltimore)*, 97(14):e0415. https://doi.org/10.1097/MD.0000000000010415

List of electronic supplementary materials

Table S1 Full list of microarray-based HUVEC hypoxia/re-oxygenation-induced differentially regulated gene probes

中文概要

题　目：基于微阵列技术的缺氧/复氧诱导下血管内皮细胞转录组分析

目　的：应用全转录组芯片研究缺氧/复氧诱导下人脐静脉内皮细胞（HUVEC）的转录组轮廓。

创新点：血管内皮细胞（VEC）缺氧/复氧损伤被视定为许多生理和病理过程中导致器官功能障碍的重要驱动因素。然而，其详细病理生理机制和基因表达谱信息尚未阐明。本研究首次应用全转录组芯片技术研究 VEC 缺氧/复氧诱导下的转录组轮廓。

方　法：采用缺氧孵育 3 h 后复氧 1 h 的 HUVEC 为缺氧/复氧组，同时常氧孵育的 HUVEC 为常氧对照组。应用含 58 339 条探针的全转录组芯片检测每组三个样本。对差异表达基因进行生信分析和功能验证。

结　论：本研究发现 372 个有意义的差异表达基因探针。相关基因涵盖多种途径和功能，例如氧自由基的产生、钙超载、炎症、糖脂代谢、内皮细胞增殖、分化、细胞骨架及通透性调节、细胞裂解、凋亡和血管生成。另外，实验进一步表明，差异表达基因 pleckstrin 同源样域家族 A 成员 1（PHLDA1）的 mRNA 和蛋白质表达结果与微阵列结果一致。STRING 分析发现，*PHLDA1* 可能与差异表达基因 *SLC38A3*、*SLC5A5*、*Lnc-SLC36A4-1* 和 *Lnc-PLEKHJ1-1* 具有物理性和/或功能性相互作用，这有望揭示 VEC 在缺氧/复氧环境下长链非编码 RNA（lncRNA）的相关机制。

关键词：人脐静脉内皮细胞；缺氧；复氧；微阵列；PHLDA1；长链非编码 RNA